



Research Article

Antioxidant Activity of Lawsone and Prediction of its Activation Property on Superoxide Dismutase

¹Muhammad Noorfaiz Mohd Noor, ²Shazleen Sofea Abdullah, ¹Hasiah Ab Hamid, ³Muhammad Alif Mohammad Latif and ^{1,2}Siti Farah Md Tohid

¹Department of Biomedical Science, Faculty of Medicine and Health Sciences, Universiti Putra Malaysia, Selangor, Malaysia

²Halal Product Research Institute, Universiti Putra Malaysia, Selangor, Malaysia

³Department of Chemistry, Faculty of Science, Universiti Putra Malaysia, Selangor, Malaysia

Abstract

Background and Objective: Lawsone, from *Lawsonia inermis* is reported with high antioxidant properties and is predicted to reduce oxidative stress via binding to the domain of oxidative enzyme Superoxide Dismutase (SOD) receptor. This study is intended to evaluate lawsone's total antioxidant activity *in vitro* and the SOD activation property *in silico*. **Materials and Methods:** Cytotoxicity of lawsone on A431 and 3T3 cell lines was obtained via MTT assay. Next, FRAP assay was carried out in 2 conditions *in vitro*: (a) In the absence of cells, and (b) At 200 μM in A431 and 3T3 cells to assess the total antioxidant activity. For *in silico* studies, AlloSite 2.0 webserver was used to predict the SOD's allosteric site, followed by AutoDock Tools (ADT) for molecular docking and finally interaction analysis via PyMOL software, ProteinsPlus and PLIP webserver. **Results:** IC_{50} of lawsone on the A431 cell line was determined at 3650 μM while no IC_{50} was detected on the 3T3 cell line. Lawsone exhibited the total antioxidant activities in the absence of cells, in A431 and 3T3 cell lines at 4.04 ± 0.18 , 94.41 ± 1.21 and 93.50 ± 8.48 μM , respectively. *In silico* results showed that lawsone binds to 2 allosteric regions A and B of SOD1, with binding affinities of -7.3 and -6.6 kcal mol^{-1} , respectively. Molecular docking results illustrated several hydrophobic interactions and 4 hydrogen bondings between lawsone and SOD. **Conclusion:** Lawsone exhibited a low range increment in total antioxidant activity at low concentration and can excellently bind to the allosteric sites of SOD.

Key words: Lawsone, anti-inflammatory, antioxidant, FRAP assay, superoxide dismutase, molecular docking, allosteric site

Citation: Noor, M.N.M., S.S. Abdullah, H.A. Hamid, M.A.M. Latif and S.F.M. Tohid, 2022. Antioxidant activity of lawsone and prediction of its activation property on superoxide dismutase. *Int. J. Pharmacol.*, 18: XX-XX.

Corresponding Author: Siti Farah Md Tohid, Department of Biomedical Science, Faculty of Medicine and Health Sciences, Universiti Putra Malaysia, Selangor, Malaysia

Copyright: © 2022 Muhammad Noorfaiz Mohd Noor *et al.* This is an open access article distributed under the terms of the creative commons attribution license, which permits unrestricted use, distribution and reproduction in any medium, provided the original author and source are credited.

Competing Interest: The authors have declared that no competing interest exists.

Data Availability: All relevant data are within the paper and its supporting information files.

INTRODUCTION

Free radicals are unstable molecular species that contain unpaired electrons in their outer shell and can exist on their own, whereas the Reactive Oxygen Species (ROS) is a term that is used to include the free radicals and non-radicals such as singlet oxygen, peroxy nitrite and hydrogen peroxide^{1,2}. All aerobic organisms generate and eliminate reactive oxygen species, resulting in either the physiological amount needed for regular cell function or unsustainable amounts, a phenomenon called oxidative stress. Oxidative stress is the term that refers to the inequity between the production of ROS and the production of the protective antioxidant². Oxidative stress can cause inflammation on the skin³. Oxidative stress has already been shown as the primary mechanism of various diseases as the correlation between oxidative stress, particularly in lipid peroxidation and different inflammatory skin condition such as atopic dermatitis and psoriasis has been shown by compelling evidence⁴.

Thus, some compounds, known as antioxidants, can protect the skin from free radicals. They are naturally occurring antioxidants in our skin that protect cells and tissue during normal metabolism from the continuous development of reactive oxygen metabolites, which consists of enzymatic and non-enzymatic antioxidants. Enzymatic antioxidants act as the first line of defence, for instance, Glutathione Peroxidase (GPx), Superoxide Dismutase (SOD) and Catalase (CAT) while non-enzymatic antioxidants such as metal chelating agent, binds to the redox-active metals and suppress the production of metal-catalysed free radicals⁵. Superoxide Dismutase (SOD) is the primary antioxidant defence system by catalysing the conversion of superoxide anion and hydrogen peroxide participating in cell signalling at each subcellular location. SOD also plays a crucial role in suppressing oxidative inactivation of nitric oxide, thereby preventing the production of peroxy nitrite and endothelial and mitochondrial impairment⁶.

Nowadays, a lot of studies prove that compounds from natural products act as an antioxidant, which can give protection from inflammation to the skin. The extracts of *Lawsonia inermis*, commonly known as Henna, are among the most frequently used skin dyes⁷. Henna has been widely used in traditional medicine to treat inflammation, cancer, bacterial and fungal infections and various skin ailments⁸. The primary active component of *L. inermis* is lawsone or 2-hydroxy-1,4-naphthoquinone (Fig. 1). A lot of studies have proven that lawsone possesses several remarkable biological functions, such as antioxidant, antibacterial and antifungal, anti-inflammatory, antipyretic and analgesic and anticancer⁹. Thus, the present study aims to evaluate the total antioxidant

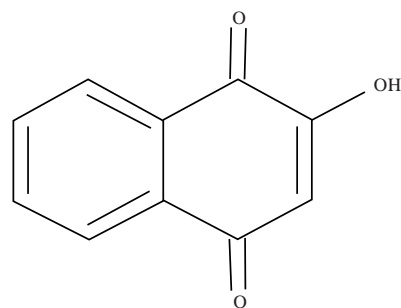


Fig. 1: Structure of lawsone (2-hydroxy-1,4-naphthoquinone)

activity of lawsone *in vitro* and the SOD activation property of lawsone *in silico*. It is expected that lawsone may exhibit good total antioxidant activity via Ferric Reducing Antioxidant Power (FRAP) assay and have an excellent binding affinity at the allosteric sites of SOD *in silico* which is can simultaneously trigger the activation of the SOD enzyme.

MATERIALS AND METHODS

Study area: The studies were carried out at the Department of Biomedical Science, Faculty of Medicine and Health Sciences, Universiti Putra Malaysia, from January-August, 2020.

In vitro assays

Chemicals: Dulbecco's Modified Eagle Media (DMEM) culture media, penicillin-streptomycin, trypsin, Ethylene Diamine Tetraacetic Acid (EDTA), 3-(4,5-dimethylthiazol-2-yl)-2,5-diphenyl tetrazolium bromide (MTT) were obtained from Nacalai Tesque Inc. (Kyoto, Japan). Phosphate Buffer Solution (PBS) was purchased from 1st Base (The Gemini, Singapore). Fetal Bovine Serum (FBS), trypan blue solution 0.4%, 2,4,6-tripyridyl-s-triazine (TPTZ), ferrous sulphate heptahydrate (FeSO₄·7H₂O) and sodium acetate anhydrous were acquired from Sigma-Aldrich (St. Louis, Missouri, USA). Dimethyl Sulfoxide (DMSO) and glacial acetic acid were purchased from AMRESCO (Solon, Ohio, USA). Hydrochloric acid (HCl) and Ferric Chloride Hexahydrate (FeCl₃·6H₂O) were purchased from Fisher Scientific (Loughborough, Leicestershire, UK). L-ascorbic acid was obtained from Santa Cruz Biotechnology (Dallas, TX, USA) and sodium hydroxide (System, Classic Chemicals, Shah Alam, Selangor, Malaysia). The powdered form of lawsone (2-hydroxy-1,4-naphthoquinone) was purchased from Sigma-Aldrich (St. Louis, MO, USA).

Cell culture: Human epidermoid carcinoma (A431) was a generous gift from Prof. Dr. Tan Wen Siang from Faculty of Biotechnology, Universiti Putra Malaysia and normal mouse

fibroblast (3T3) cell lines were purchased from American Type Culture Collection (ATCC). All the cell lines were cultured in the culture flasks containing DMEM culture media, FBS and penicillin-streptomycin with the percentage of 89, 10 and 1%, respectively, using 44.5 mL of DMEM culture media, 5 mL of FBS and 500 μ L of penicillin-streptomycin. The confluence of the cells was observed under the phase-contrast inverted microscope before subculturing in fresh media after washing with Phosphate-Buffered Saline (PBS) and trypsinisation. Cell viability was observed by using trypan blue staining before cell seeding for cytotoxicity and FRAP assays.

Cytotoxicity assay: The growth and cytotoxicity of cells were determined by MTT assay¹⁰. About 100 μ L of A431 and 3T3 cell lines were seeded into separate 96-well plates with the seeding density of 1×10^5 cells mL^{-1} . The plates were then incubated at 37°C in a 5% CO₂ incubator for 24 hrs. The working solution of lawsone and DMEM media were prepared in sterile Petri dishes. After 24 hrs, the cells in both plates were treated with 100 μ L of lawsone with 10 different concentrations (5000, 2500, 1250, 625, 312.5, 156.75, 78.13, 39.07, 19.53 and 9.77 μ M). The well with complete media growth and without lawsone treatment was acted as the negative control. The plates were then wrapped with aluminium foil and incubated at 37°C in a 5% CO₂ incubator for 48 hrs. The MTT solution (5 mg mL^{-1}) was prepared by dissolving into PBS solution. After 48 hrs incubation, 20 μ L of MTT solution was added to each well of the 96-well plate. The plates were wrapped with aluminium foil and incubated at 37°C in a 5% CO₂ incubator. After 4 hrs of incubation, the medium of the wells was aspirated and 100 μ L of DMSO was replaced into each well. The plate was then read using a microplate reader (Infinite F50, Tecan, Männedorf, Switzerland) with a wavelength of 570 nm and a reference wavelength of 630 nm after a shake for 10 sec. A graph of cell viability against lawsone concentration was plotted. IC₅₀ was determined from the concentration versus cytotoxicity graph. The cytotoxicity was calculated based on the formula¹¹:

$$\text{Cytotoxicity (\%)} = \frac{\text{Optical density of sample (mean)}}{\text{Optical density of control (mean)}} \times 100$$

Ferric reducing antioxidant power (FRAP) assay: The method from Faria *et al.*¹² was used to perform biochemical FRAP assay, while a few modifications were performed as reported by Hasiyah *et al.*¹³ to perform FRAP assay in cell lines. Both A431 and 3T3 cell lines were plated as in MTT assay in a 96-well plate with the seeding density of 1×10^4 cells mL^{-1} .

The plates then were incubated at 37°C in a 5% CO₂ incubator for 24 hrs. Then, the cells in both plates were treated with 50 μ L of lawsone with eight different concentrations (200, 100, 50, 25, 12.5, 6.25, 3.13 and 1.56 μ M). The positive control used in this assay was vitamin C (L-ascorbic acid). The plates were then wrapped with aluminium foil and incubated at 37°C in a 5% CO₂ incubator for 24 hrs. Then, the plates were sonicated by using the sonicator (Powersonic 410, Hwashin Technology Co., Seoul, South Korea) for 30 sec. The plates were added with 150 μ L of freshly prepared FRAP reagent which was warmed at 37°C. The plates were then read on a fluorescence microplate reader (Infinite 200 Pro, Tecan, Männedorf, Switzerland) with a wavelength of 593 nm. The absorbance reading was converted into a FRAP value (μ M). The biochemical FRAP assay on lawsone without the presence of the cell lines was also performed by adding FRAP reagent immediately to the lawsone solution in a 96-well plate. The series of Ferrous Sulphate Heptahydrate (FeSO₄·7H₂O) concentrations from 100-1000 μ M was prepared for obtaining the standard curve.

Statistical analysis: *In vitro* results were analysed by using Analysis of Variance (ANOVA), followed by Dunnett's test as a post hoc test, which is significant at $p < 0.05$. All of this was analysed by using the software package of IBM SPSS Statistical Package Version 26.

In silico studies

Determination of allosteric site: The SOD protein was retrieved from the RSCB protein data bank in the .pdb format file with PDB ID of 2C9V, atomic resolution of Cu-Zn human superoxide dismutase with a resolution of 1.07Å. All chains of 2C9V (chain "A" and "F") were selected to determine the possible allosteric sites by using AlloSite Version 2.10 webserver¹⁴. The report of results was downloaded and the PDB file of the allosteric prediction site of 2C9V was observed by using PyMOL software.

Preparing receptor and ligand input: AutoDock Tools (ADT) and AutoDock Vina were used to evaluate and perform molecular docking¹⁵. PDB ID of 2C9V of SOD receptor was acquired from RSCB Protein Data Bank in the '.pdb' file. Meanwhile, as for the ligand, the structure of lawsone was retrieved in '.sdf' format from PubChem which was then converted to '.pdb' format by using open babel software. Both SOD and lawsone were required to be prepared into PDBQT format for the AutoDock Vina to evaluate and perform the molecular docking. Next, the hydrogen atoms were added and

Table 1: Adjusted parameters were used to set up the docking grid box for SOD

Protein	Area	Grid size		Grid coordinate	
SOD	A	x	14	x	12.407
		y	30	y	-4.285
		z	18	z	11.315
	B	x	8	x	32.034
		y	12	y	-0.611
		z	8	z	17.785

merged with the polar and non-polar hydrogens. The charges were computed using the Gasteiger method. The torsion was then assigned to the ligand.

Setting up docking grid box and configuration files: Table 1 shows the adjusted parameters used for docking of SOD. The grid box size and coordinates were identified to operate as molecular docking parameters. The parameters above were written in a text editor such as Notepad or Crimson Editor and saved as a configuration file in '.txt' format.

Molecular docking via AutoDock Vina: The molecular docking between lawsone and SOD was carried out by utilizing AutoDock Vina software¹⁶. The prepared PDB files of SOD and lawsone, the configuration file in '.txt' format and AutoDock Vina software were included in 1 folder before proceeding to the command prompt for running the docking job.

Analysis on docked complexes: The docked ligand conformation produced the 9 best results of binding affinity with different pose predictions between the lawsone and SOD. Thus, the best-docked ligand-protein complex (lawsone-SOD complex) with top binding affinity was then analysed by using PyMOL software (PyMOL Molecular Graphics System, Version 2.3 Schrödinger, LLC.), ProteinsPlus (Zentrum für Bioinformatik: Universität Hamburg-Proteins Plus Server) and PLIP webserver (Protein-Ligand Interaction Profiler, Biotechnology Center TU Dresden). The two-dimensional (2D) information of the interaction between the docked lawsone-SOD complex was obtained from ProteinsPlus.

RESULTS

In vitro analysis

Effect of lawsone on cell cytotoxicity: MTT assay was used to determine the toxicity profile of lawsone in the cells. Thus, IC_{50} was obtained to determine the cytotoxicity of lawsone on the epidermoid A431 and fibroblast 3T3 cell lines. The cells were treated with various dosage ranges of concentration from

5000, 2500, 1250, 625, 312.5, 156.75, 78.13, 39.07, 19.53, 9.77 and 0 μ M. The incubation time of the treatment was 24 hrs. The data in Fig. 2a showed the cytotoxicity result of lawsone on the percentage of cell viability of epidermoid A431 at various groups of treatments. By using the graph as a reference, the lawsone IC_{50} was determined at 3650 μ M. Meanwhile, Fig. 2b showed the cytotoxicity result of lawsone on the percentage of cell viability of fibroblast 3T3 at various groups of treatments. By using the graph as a reference, no IC_{50} was detected for lawsone below the concentration of 5000 μ M. The value of IC_{50} was then used as the reference dose for the preceding FRAP assay.

Total antioxidant activity (biochemical FRAP assay-absence of cells): Biochemical FRAP assay was used to determine the total antioxidant activity of vitamin C (Fig. 3a, as the positive control) and lawsone (Fig. 3b). A various dosage range of vitamin C and lawsone concentrations from 200, 100, 50, 25, 12.5, 6.25, 3.13, 1.56 and 0 μ M were utilized for the FRAP assay.

Total antioxidant activity on cell lines: Cell line-based FRAP assay was used to determine the total antioxidant activity of lawsone and vitamin C on both cell lines, namely epidermoid A431 cell line (Fig. 4a) and fibroblast 3T3 cell line (Fig. 4b). The cells were treated with a various dosage range of concentrations from 200, 100, 50, 25, 12.5, 6.25, 3.13, 1.56 and 0 μ M.

In silico analysis

Crystal structure and hydrophobic pocket residues of SOD: The SOD receptor (PDB ID of 2C9V) was acquired from RSCB Protein Data Bank (Fig. 5). The crystal structure consisted of 2 chains known as chains A and F with 4 ligand molecules, copper (Cu), sodium (Na), sulfate (SO_4) and zinc (Zn) which were attached to the hydrophobic pocket of SOD. SOD is a dimer that consists of only chain A, while, chain F is an exact copy of the latter. However, both chains were needed for this molecular docking study as the allosteric site was yet to determine in both chains.

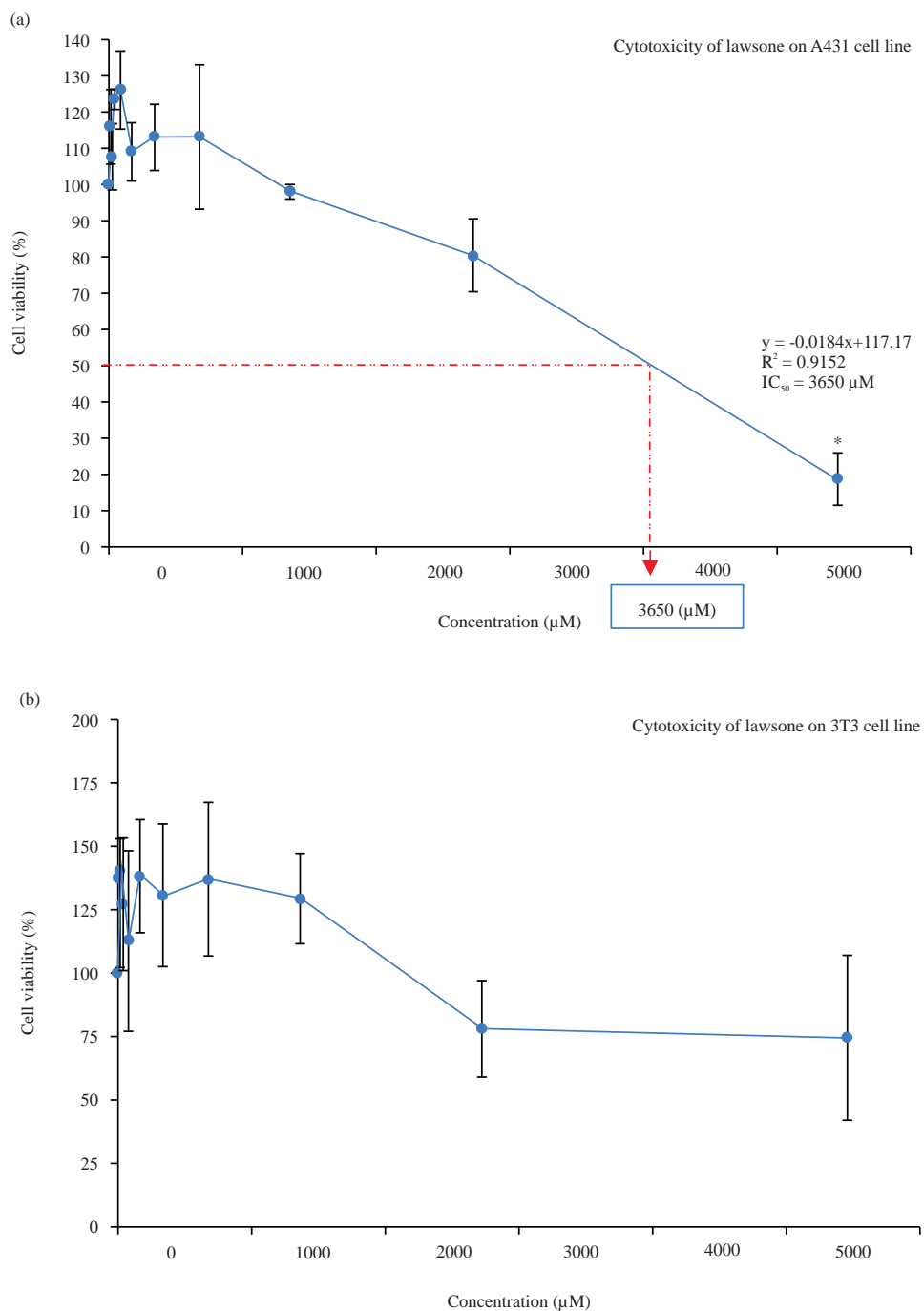


Fig.2(a-b): Graph of cell viability at various concentrations of lawsone treatment towards the (a) A431 and (b) 3T3 cell lines

Cell viability of epidermoid A431 and 3T3 fibroblast cell lines after being treated with lawsone of various concentrations (5000, 2500, 1250, 625, 312.5, 156.75, 78.13, 39.07, 19.53, 9.77 and 0 µM) in 24 hrs. The values were expressed as Mean ± SEM from 3 independent experiments, where * was indicated the significant difference ($p < 0.05$) relative to the untreated cells, one-way ANOVA was used to perform the statistical analysis followed by Dunnett's test as the *post-hoc* test

Determination of allosteric sites of SOD: Allosteric sites of SOD was determined by using AlloSitePro 2016. By using AlloSitePro 2016, a possible allosteric site in SOD can be

predicted. The data in Fig. 6 below showed the potential regions (green spheres) of the allosteric site in SOD, namely region A and region B.

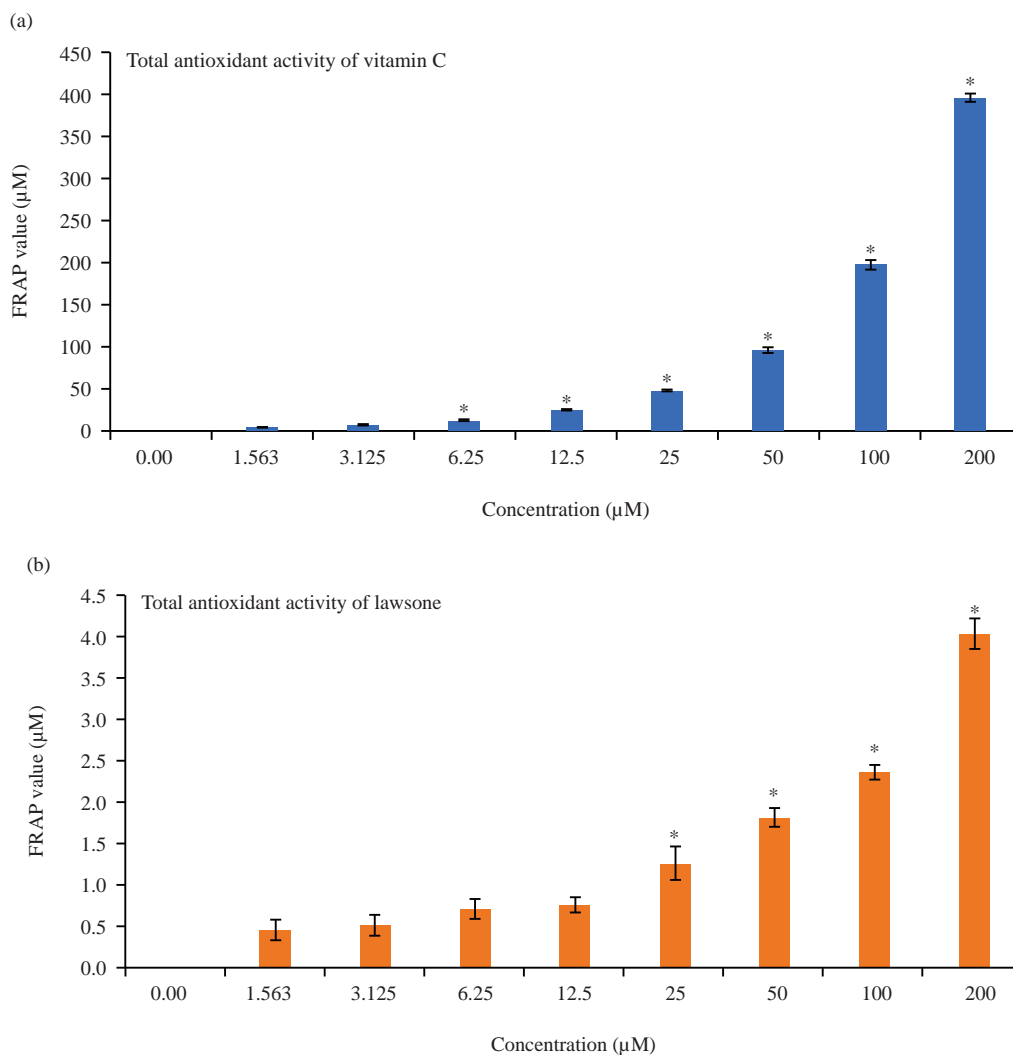


Fig. 3(a-b): Graph of the total antioxidant activity of (a) Vitamin C and (b) Lawsone in the absence of cells

Total antioxidant activity of vitamin C and lawsone with various concentrations (200, 100, 50, 25, 12.5, 6.25, 3.13, 1.56 and 0 µM), data were represented as Mean ± SEM from 3 independent experiments, where *was indicated the significant difference ($p < 0.05$) relative to the control group, one-way ANOVA was used to perform the statistical analysis followed by Dunnett's test as the *post-hoc* test

Table 2: Predicted binding modes of lawsone to SOD (region A)

Modes	Binding affinity (kcal mol ⁻¹)
1	-7.3
2	-7.2
3	-7.1
4	-6.9
5	-6.9
6	-6.8
7	-6.8
8	-6.8
9	-6.7

AutoDock Vina result: AutoDock Vina predicted the 9 best binding modes between lawsone and SOD as the poses were arranged into ranking from the highest binding affinity to lowest binding affinity. The best-docked configuration with the highest binding affinity was selected for further analysis.

Table 2 and 3 showed the results of molecular docking between lawsone and SOD for region A and B, respectively.

Analysis of best docked complexes: AutoDock Vina predicted the 9 best binding modes between lawsone and SOD as the poses were arranged into ranking from the highest binding affinity to lowest binding affinity. The best-docked configuration with the highest binding affinity was selected for further analysis. Table 2 and 3 showed the results of molecular docking between lawsone and SOD for region A and B, respectively.

Region A: Lawsone bind to the region A of the allosteric site of SOD with the highest binding affinity at $-7.3 \text{ kcal mol}^{-1}$. The

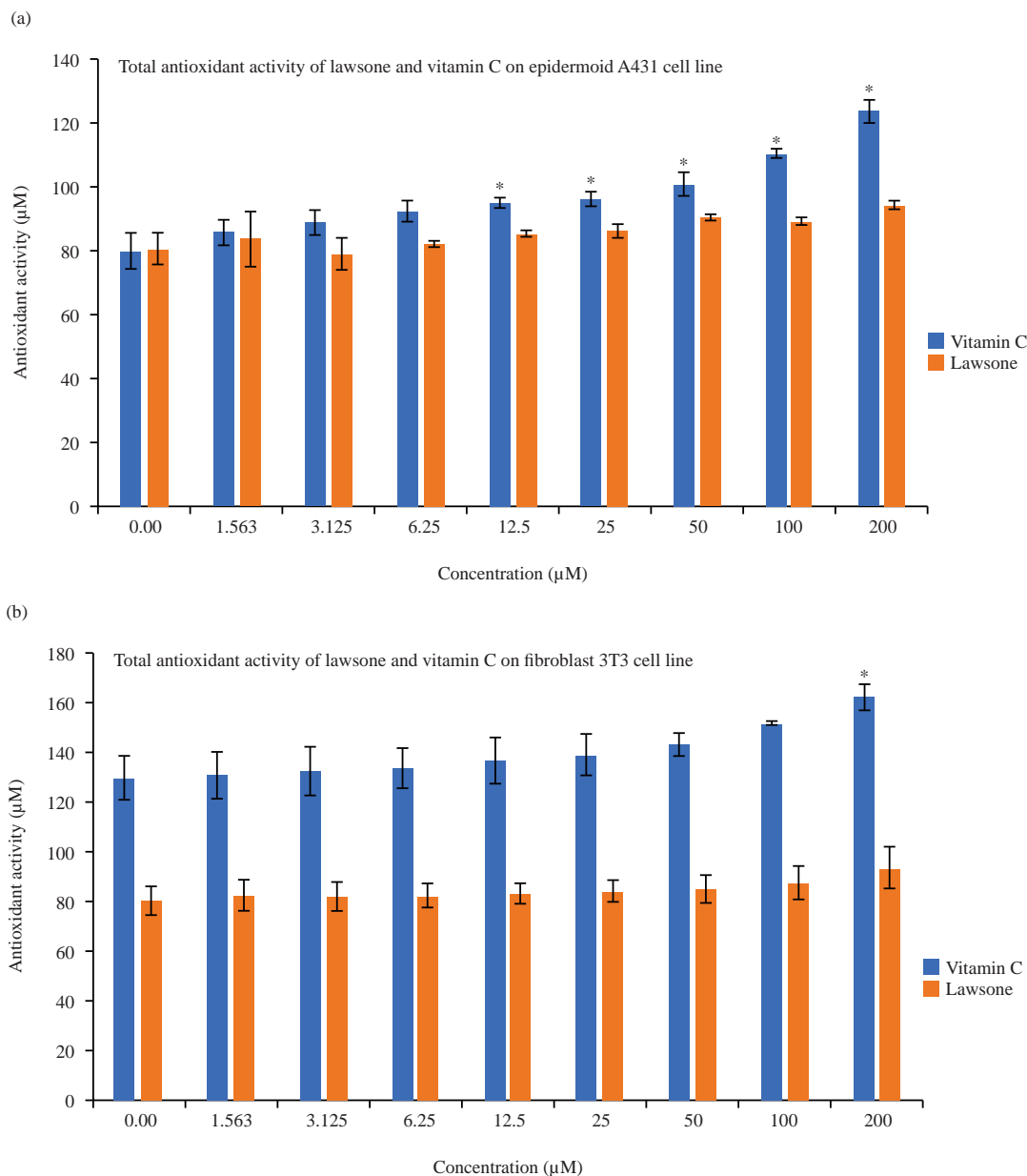


Fig. 4(a-b): Graph of the total antioxidant activities of vitamin C and lawsone at various concentrations on (a) Epidermoid A431 cell line and (b) Fibroblast 3T3 cell line

Total antioxidant activity of A431 epidermoid and 3T3 fibroblast cell line after being treated with vitamin C and lawsone of various concentrations (5000, 2500, 1250, 625, 312.5, 156.75, 78.13, 39.07, 19.53, 9.77 and 0 μM), data were represented as Mean ± SEM from 3 independent experiments, where *was indicated the significant difference ($p < 0.05$) relative to the control group, one-way ANOVA was used to perform the statistical analysis followed by Dunnett's test as the *post-hoc* test

2D result was analysed by using ProteinsPlus (Fig. 7a). Two hydrogen bonds were formed between the hydroxyl group (distance 2.82Å) and a carbonyl group (distance 1.91Å) of lawsone and amide group of Valine 148 (Val148) residue at chain A.

The 3D result was obtained from the PLIP webserver (Fig. 7b). There were 6 hydrophobic interactions between

residues of SOD and lawsone. The hydrophobic interactions were formed between the aromatic ring of lawsone and the hydrophobic pockets of Valine 7 (Val7), Lysine 9 (Lys9) residues at chain F and Asparagine 53 (Asn53) residue at chain A. There was also hydrophobic interactions between the hydrophobic pockets of Asparagine 53 (Asn53) and Valine 148 (Val148) residues at chain F and the carbonyl group of

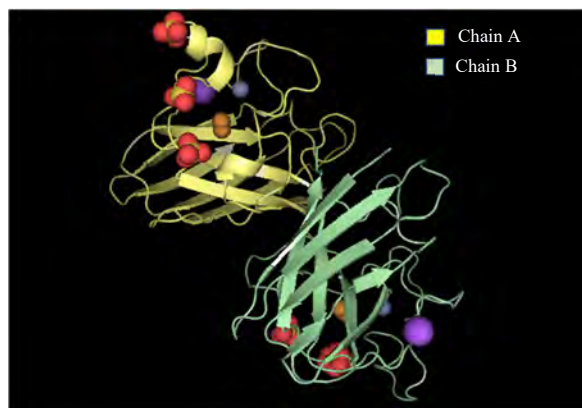


Fig. 5: Crystal structure of SOD retrieved from PDB (ID: 2C9V)

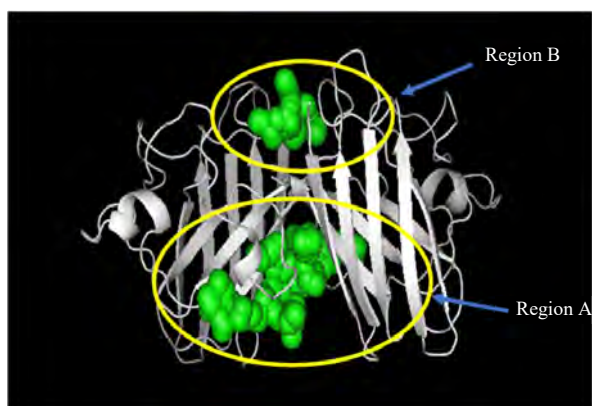


Fig. 6: Allosteric sites of SOD

Table 3: Predicted binding modes of lawsone to SOD (region B)

Modes	Binding affinity (kcal mol ⁻¹)
1	-6.6
2	-6.6
3	-6.5
4	-6.4
5	-6.3
6	-6.2
7	-6.2
8	-6.2
9	-6.2

lawsone. Simultaneously, a hydrogen bond was also established between the carbonyl group of lawsone and Valine 148 (Val148) residue at chain A. Fig. 7c illustrated the binding pose of lawsone embedded into the hydrophobic groove of SOD in region A.

Region B: Lawsone bind to the region B of the allosteric site of SOD with the highest binding affinity at -6.6 kcal mol⁻¹. The 2D result was analysed by using ProteinsPlus (Fig. 8a). There was a presence of a hydrophobic pocket of Isoleucine 113 (Ile113) residue from chain A at the aromatic ring of

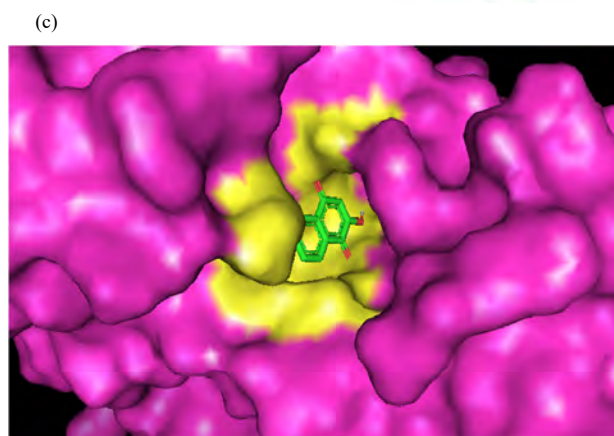
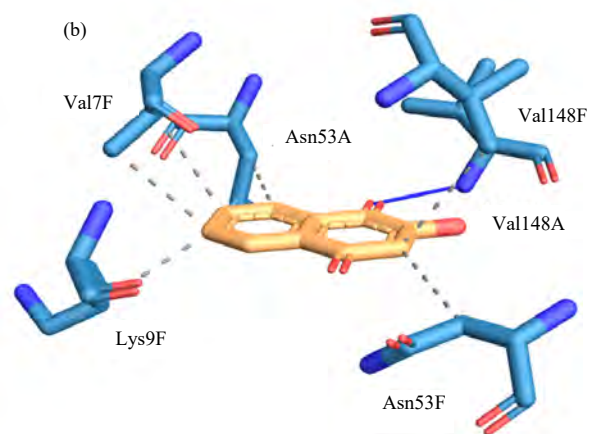
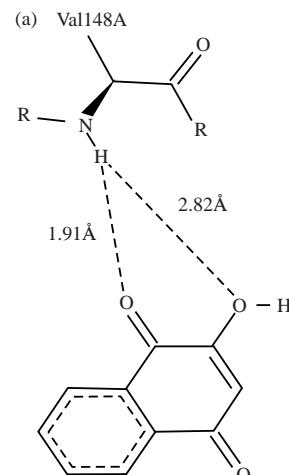


Fig. 7(a-c): Best-docked complex between lawsone and SOD from region A, (a) Lawsone interacts with Valine 148 residue at chain A, (b) Hydrophobic interactions (grey dashed line) and hydrogen bonding (blue line) between residues of SOD and lawsone were analysed by using the PLIP webserver and (c) View from PyMOL of lawsone best binding pose on SOD

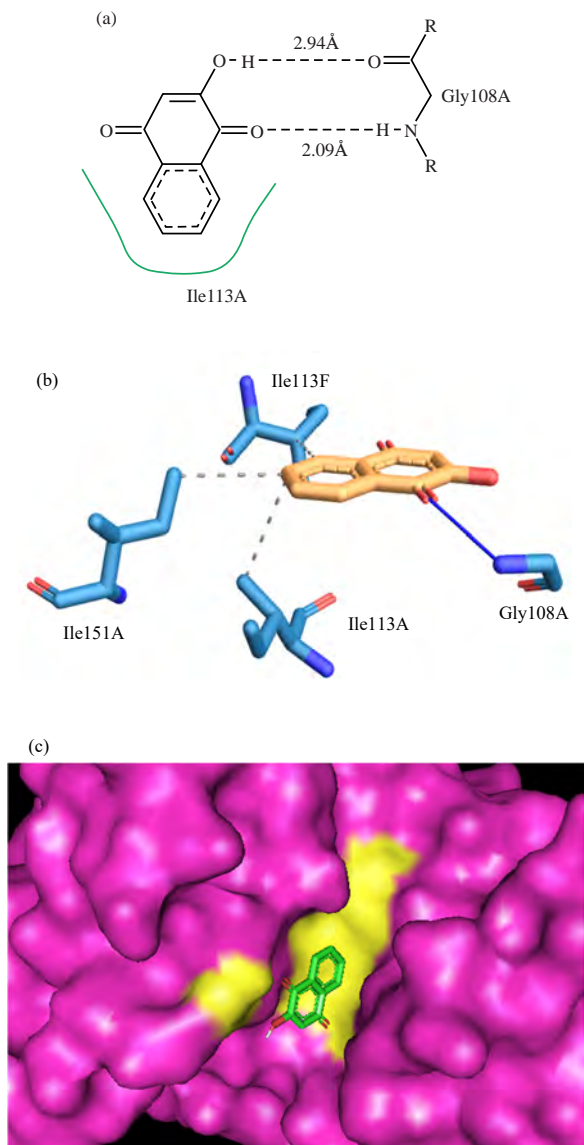


Fig. 8(a-c): Best-docked complex between lawsone and SOD from region B, (a) Lawsone interacts with Isoleucine 113 and Glycine 108 residues at chain A, (b) Hydrophobic interactions (grey dashed line) and hydrogen bonding (blue line) between residues of SOD and lawsone were analysed by using the PLIP webserver and (c) View from PyMOL of lawsone best binding pose on SOD

lawsone. Concurrently, 2 hydrogen bonds were formed between the carbonyl group (distance 2.09Å) and a hydroxyl group (distance 2.94Å) of lawsone and amide group and the carbonyl group of Glycine 108 (Gly108) residue at chain A, respectively.

The 3D result was obtained from the PLIP webserver (Fig. 8b). There were 3 hydrophobic interactions between

residues of SOD and lawsone. The hydrophobic interactions were formed between the aromatic ring of lawsone and the hydrophobic pockets of Isoleucine 113 (Ile113), Isoleucine 151 (Ile151) residues at chain A and Isoleucine 113 (Ile113) residue at chain F. Simultaneously, a hydrogen bond was also established between the carbonyl group of lawsone and Glycine 108 (Gly108) residue at chain A. Fig. 8c illustrated the binding pose of lawsone embedded into the hydrophobic groove of SOD in region B.

DISCUSSION

Firstly, the study assessed the cytotoxicity of lawsone on A431 and 3T3 cell lines. The cytotoxicity of lawsone on both cell lines was determined by the IC_{50} values. The IC_{50} value of lawsone obtained from the graphs indicated that the cytotoxic effect of lawsone only occurs at high concentrations. This demonstrated lawsone as a valuable candidate for potential antioxidant agents as it has low cytotoxic characteristics. This was supported by Lozza *et al.*¹⁷ which reported that lawsone offered the clinical potential for managing skin conditions defined by hyperproliferation and inflammation, owing to its low cell toxicity. IC_{50} of lawsone from both cells was later used as a reference dose to determine the suitable range of concentration of lawsone for the preceding FRAP assay.

Next, lawsone was used to determine the total antioxidant activity in 2 settings, firstly without cell lines and secondly with the presence of cell lines which were A431 and 3T3 cell lines by using FRAP assay. The total antioxidant activity of lawsone increased in a concentration-dependent manner from the concentration of 1.56 up to 200 μ M. This was supported by Majiene *et al.*¹⁸ in their study, where the concentration range of 50-1000 μ M lawsone demonstrated a significant antioxidant activity by using dichloro-dihydro-fluorescein diacetate (DCFH-DA) assay on C6 glioblastoma cells statistically. This could be as strong supporting evidence in which lawsone possessed metal chelating and free radical scavenging features.

On the other hand, the total antioxidant activity of lawsone towards A431 and 3T3 cell lines showed an increment in concentration up to 200 μ M but in a very low range. Firstly, it might occur because the data from the result showed that there was a presence of antioxidant activities observed in the control group, utilising the untreated cell lines without lawsone treatment. It is supported by Hasiah *et al.*¹³ as they suggested that the cell lines might have their endogenous antioxidant activity. In addition, this occurrence suggested that lawsone might be metabolised into an unstable and inactive format a low concentration by both cell lines before

it can exert its biological activity. According to Yang *et al.*¹⁹, lawsone can be reduced to 1,2,4-trihydroxynaphthalene. This metabolite was relatively in an unstable form as the presence of hydroxyl cloud in the metabolite can amplify the electron cloud density of the naphthalene ring. In contrast, Osman and van Noort²⁰ suggested that lawsone is a non-redox-cycling quinone because lawsone is not a substrate for NADPH-cytochrome C reductase as such electron-transferring flavoenzymes cannot reduce lawsone and also it is considered a poor substrate for NAD(P)H: Quinone oxidoreductase₁ (NQO₁) *in vitro*. Also, Sauriasari *et al.*²¹ reported that lawsone has weak electrophilic features *in vitro*. Thus, it cannot react spontaneously due to the presence of an anionic form of lawsone itself. This caused lawsone does not undergo redox cycling *in vitro*. Another reason that could be the cause of insignificance which the 3T3 cell line displayed low saturation density, grow at high dilution and was highly sensitive to cell division inhibition after confluence although it was capable of dividing the cells indefinitely²². Thus, it is predicted that this study can be improved by increasing the concentration of lawsone when performing the cell-based FRAP assay up to 1000 μ M to observe the total antioxidant activity of lawsone in 3T3 and A431 cells lines at high concentration.

Nevertheless, many studies showed many pieces of evidence of the excellent antioxidant activity of lawsone despite the result obtained from the cell-based FRAP assay from this study. Kurtyka *et al.*²³ reported that lawsone yielded higher production of H₂O₂ and activity of antioxidative enzymes such as SODs, catalases and peroxidases in coleoptile cells when compared to the juglone, an isolated metabolite from *Juglans nigra* or black walnut tree. Meanwhile, Zohourian *et al.*²⁴ reported that, although lawsone did not mostly exert the antioxidant activity of henna but also due to the presence of other polyphenolic compounds from the extracts, pure lawsone already showed almost half of the antioxidant activity of the extract itself.

Moreover, although FRAP assay measured the potential of biological antioxidants, it also measured chemical reductant that reduced ferric complex to ferrous form, using the reduction of Fe³⁺-TPTZ to Fe²⁺-TPTZ. However, not all reductants were antioxidants such as glutathione as it cannot reduce Fe³⁺ to Fe²⁺. Therefore, FRAP assay does not justify-SH antioxidant group²⁵. This determined that the increment of ROS does not strongly interpret that there is an increment in antioxidant concentration or vice versa. Thus, an antioxidant assay such as GSH reductase assay can be done for future study to further investigate the antioxidant activity within the biological system such as in cell lines.

The next part of the study which is the *in silico* study attempted to unbridle the potential activation mechanism of lawsone towards SOD to combat the oxidative stress condition caused by ROS. A previous study described that lawsone played a significant role in the generation of hydrogen peroxide and ROS scavenger in maize coleoptile segments by increasing the antioxidant enzyme such as SOD²³.

Before proceeding with the molecular docking method, the allosteric site of SOD1 protein from the PDB (ID: 2C9V) was determined by using AlloSite 2.0. Allosite was available through the web server worldwide and it was a recently developed automatic contrivance to predict the allosteric regions in the protein of interest²⁶. Determination of the allosteric sites of SOD was done as SOD is known for its high stability in structure due to the presence of copper and zinc for redox and stabilising function, respectively²⁷. Song *et al.*¹⁴ reported that targeting and identifying allosteric sites of a protein has turned into quite an attention as a novel strategy for allosteric-targeting drug development. Binding to the allosteric site may exploit specific features which characterise target protein from other homologous proteins. Also, the structural variety of allosteric sites provides the allosteric modulators with better selectivity, fewer side effects and minor toxicity. Thus, lawsone was expected to exhibit antioxidant properties by binding to the allosteric site of SOD and enhancing the SOD activity.

After determining the allosteric sites of SOD (which are named region A and region B), lawsone was then docked to the specific hydrophobic pockets of allosteric sites of SOD. Based on the results provided by the AutoDock Vina, the docking of the lawsone-SOD complex showed a range of binding affinities from -6.7, -7.3 kcal mol⁻¹ for region A and -6.2, -6.6 kcal mol⁻¹ for region B. However, it was preferable to choose the first mode as the best predicted binding pose as the search for ligand confirmation was always towards the negative values. Higher binding affinity is signified by the negative score and weaker binding affinity is signified by the positive score from the AutoDock Vina²⁸. As for Region B, the value of Root-Mean-Square Deviation (RMSD) for the second mode was higher compared to the first mode. Lower RMSD values were correlated with a higher resolution of protein structure²⁹. Thus, the first model was chosen as the best predicted binding pose between lawsone and SOD although the second mode has the same binding affinity value as the first mode.

Next, the best binding affinity of lawsone to SOD1 from region A was recognised by the formation of hydrogen bonds between the hydroxyl group and the carbonyl group of

lawsone and amide group of Valine 148 from chain A (Val148A), along with the hydrophobic interaction at the hydrophobic pockets of Valine 7 (Val7), Lysine 9 (Lys9), Asparagine 53 (Asn53) and Valine 148 (Val148) residues at chain F and Asparagine 53 (Asn53) residue at chain A. From region B, it was recognised by the formation of hydrogen bonds between hydroxyl and carbonyl group of lawsone and amide group of Glycine 108 from chain A (Gly108), along with hydrophobic interaction with Isoleucine 113 (Ile113), Isoleucine 151 (Ile151) residues at chain A and Isoleucine 113 (Ile113) residue at chain F. The most substantial interactions between lawsone and SOD were hydrogen bonds and hydrophobic interaction or known as Van der Waals force. The binding affinities for both regions were directly correlated to the analysis of docked lawsone-SOD complex. The potential for these 2 interactions in many other proteins is greater than ionic or covalent bond interactions since numerous amino acid residues can form hydrogen or hydrophobic interactions than other kinds of interactions³⁰. Furthermore, the presence of hydrophobic interactions between lawsone and SOD indicated the binding affinity between these target-protein interfaces. From the results, the study showed several hydrophobic interactions towards SOD. The biological activity of the drug lead can be increased when the number of hydrophobic atoms in the active core of the drug-protein interface increases³¹.

Besides, 4 hydrogen bonds were detected from the binding between SOD and lawsone. The distance of hydrogen bonds in region A was 1.91 and 2.82Å meanwhile in region B, at 2.09 and 2.94Å. These mentioned distances between lawsone and the SOD consisted of moderate and strong binding interactions. The distance range of hydrogen bonding can reflect the strength of hydrogen bonds, which has been categorised into strong interaction at 2.2-2.5Å, moderate interaction at 2.5-3.2Å and weak interaction at 3.2-4.0Å³².

In a nutshell, lawsone showed a good activation effect towards superoxide dismutase enzyme to reduce oxidative stress based on the result obtained from the molecular docking analysis. The activation of the SOD enzyme could be an effective indicator to be considered as a potential therapeutic target protein to treat inflammatory diseases caused by oxidative stress such as psoriasis and eczema. Hence, the potency of lawsone to trigger the activation mechanism of SOD can be developed and further studied as a potential therapy for ROS-related inflammatory diseases. Several detailed *in silico* studies can be done such as to study the Structure-Activity Relationship (SAR) of lawsone

derivatives and molecular dynamic (MD) study to further analyze the binding interactions between lawsone and SOD.

CONCLUSION

Lawsone has the potential to be developed into a promising pharmaceutical agent with low cytotoxicity and possesses good antioxidant activity. Lawsone can show a high binding affinity to the SOD enzyme and can simultaneously enhance its antioxidative activity. This highlights the capability of lawsone as a promising therapeutic antioxidant for inflammatory reaction suppression. Further studies are needed to validate the current findings as a way to develop a lawsone-based therapeutic agent with better potency and efficacy.

SIGNIFICANCE STATEMENT

This study discovers the total antioxidant activity and the possible activation mechanism of lawsone on the SOD enzyme. As lawsone was originally isolated from *Lawsonia inermis*, a plant that had been used since ancient times for topical applications on skin and hair for both cosmeceutical and therapeutic purposes, lawsone can be regarded as a valuable therapeutic candidate with minimal toxicity for the treatment of inflammation-related disorders. The prediction of lawsone's activation mechanism on the SOD enzyme is hoped to provide a new possible theory especially to further understand and delineate lawsone's mechanistic pathway as a potential therapeutic substance with good antioxidant properties. Thus, a new theory on the total antioxidant potential and the activation of SOD enzyme by lawsone may be postulated.

ACKNOWLEDGMENTS

The authors would like to acknowledge the staff of the Faculty of Medicine and Health Sciences and Halal Product Research Institute of Universiti Putra Malaysia for their help and guidance in completing this project. This study was funded by Putra-Inisiatif Putra Siswazah Research Grant [9522300] of Universiti Putra Malaysia.

REFERENCES

1. Lobo, V., A. Patil, A. Phatak and N. Chandra, 2010. Free radicals, antioxidants and functional foods: Impact on human health. *Pharmacogn. Rev.*, 4: 118-126.

2. Poljšak, B. and R. Dahmane, 2012. Free radicals and extrinsic skin aging. *Dermatol. Res. Pract.*, Vol. 2012. 10.1155/2012/135206.
3. Okayama, Y., 2005. Oxidative stress in allergic and inflammatory skin diseases. *Curr. Drug Target Inflammation Allergy*, 4: 517-519.
4. Braconi, D., G. Bernardini and A. Santucci, 2010. Post-genomics and skin inflammation. *Mediators Inflammation*, Vol. 2010. 10.1155/2010/364823.
5. Conner, E.M. and M.B. Grisham, 1996. Inflammation, free radicals and antioxidants. *Nutrition*, 12: 274-277.
6. Fukai, T. and M. Ushio-Fukai, 2011. Superoxide dismutases: Role in redox signaling, vascular function and diseases. *Antioxid. Redox Signaling*, 15: 1583-1606.
7. Jain, V.C., D.P. Shah, N.G. Sonani, S. Dhakara and N.M. Patel, 2010. Pharmacognostical and preliminary phytochemical investigation of *Lawsonia inermis* L. leaf. *Romanian. J. Biol. Plant Biol*, 55: 127-133.
8. Pradhan, R., P. Dandawate, A. Vyas, S. Padhye and B. Biersack *et al.*, 2012. From body art to anticancer activities: Perspectives on medicinal properties of henna. *Curr. Drug Targets*, 13: 1777-1798.
9. de Oliveira, A.S., I.M.C. Brighente, R.G. Lund, L.C. Llanes and R.J. Nunes *et al.*, 2017. Antioxidant and antifungal activity of naphthoquinones dimeric derived from lawsone. *J. Biosci. Med.*, 05: 39-48.
10. Cuadrado, I., F. Cidre, S. Herranz, A. Estevez-Braun, B. de las Heras and S. Hortelano, 2012. Labdanolic acid methyl ester (LAME) exerts anti-inflammatory effects through inhibition of TAK-1 activation. *Toxicol. Appl. Pharmacol.*, 258: 109-117.
11. Artun, F.T., A. Karagoz, G. Ozcan, G. Melikoglu, S. Anil, S. Kultur and N. Sutlupinar, 2016. *In vitro* anticancer and cytotoxic activities of some plant extracts on HeLa and Vero cell lines. *J. BUON*, 21: 720-725.
12. Faria, A., J. Oliveira, P. Neves, P. Gameiro, C. Santos-Buelga, V. de Freitas and N. Mateus, 2005. Antioxidant properties of prepared blueberry (*Vaccinium myrtillus*) extracts. *J. Agric. Food Chem.*, 53: 6896-6902.
13. Hasiah, A.H., A.R. Ghazali, J.F.F. Weber, S. Velu, N.F. Thomas and S.H. Inayat-Hussain, 2011. Cytotoxic and antioxidant effects of methoxylated stilbene analogues on HepG2 hepatoma and Chang liver cells: Implications for structure activity relationship. *Hum. Exp. Toxicol.*, 30: 138-144.
14. Song, K., X. Liu, W. Huang, S. Lu, Q. Shen, L. Zhang and J. Zhang, 2017. Improved method for the identification and validation of allosteric sites. *J. Chem. Inf. Model.*, 57: 2358-2363.
15. Seeliger, D. and B.L. de Groot, 2010. Ligand docking and binding site analysis with PyMOL and AutoDock/Vina. *J. Comput. Aided Mol. Des.*, 24: 417-422.
16. Trott, O. and A.J. Olson, 2010. AutoDock Vina: Improving the speed and accuracy of docking with a new scoring function, efficient optimization and multithreading. *J. Comput. Chem.*, 31: 455-461.
17. Lozza, L., P. Moura-Alves, T. Domaszewska, C.L. Crespo and I. Streata *et al.*, 2019. The henna pigment lawsone activates the aryl hydrocarbon receptor and impacts skin homeostasis. *Sci. Rep.*, 9: 1-21.
18. Majiene, D., J. Kuseliauskyte, A. Stimbirys and A. Jekabsone, 2019. Comparison of the effect of native 1,4-naphthoquinones plumbagin, menadione and lawsone on viability, redox status and mitochondrial functions of C6 glioblastoma cells. *Nutrients*, Vol. 11. 10.3390/nu11061294.
19. Yang, L., T. Cai, D. Ding, T. Cai and C. Jiang *et al.*, 2017. Biodegradation of 2-hydroxyl-1,4 naphthoquinone (lawsone) by *Pseudomonas Taiwanensis* LH-3 isolated from activated sludge. *Sci. Rep.*, Vol. 7. 10.1038/s41598-017-06338-1.
20. Osman, A.M. and P.C.M. van Noort, 2003. Evidence for redox cycling of Lawsone (2-hydroxy-1,4-naphthoquinone) in the presence of the hypoxanthine/xanthine oxidase system. *J. Appl. Toxicol.*, 23: 209-212.
21. Sauriasari, R., D.H. Wang, Y. Takemura, K. Tsutsui and N. Masuoka *et al.*, 2007. Cytotoxicity of lawsone and cytoprotective activity of antioxidants in catalase mutant *Escherichia coli*. *Toxicology*, 235: 103-111.
22. Nakamura, H., 2013. BALB/c Mouse. In: *Brenner's Encyclopedia of Genetics*, Maloy, S. and K. Hughes (Ed.), Elsevier, Amsterdam, Netherlands, ISBN-13: 9780123749840, pp: 290-292.
23. Kurtyka, R., W. Pokora, Z. Tukaj and W. Karcz, 2016. Effects of juglone and lawsone on oxidative stress in maize coleoptile cells treated with IAA. *AoB Plants*, Vol. 8. 10.1093/aobpla/plw073.
24. Zohourian, T.H., A.T. Quitain, M. Sasaki and M. Goto, 2011. Polyphenolic contents and antioxidant activities of *Lawsonia inermis* leaf extracts obtained by microwave-assisted hydrothermal method. *J. Microwave Power Electromagn. Energy*, 45: 193-204.
25. Griffin, S.P. and R. Bhagooli, 2004. Measuring antioxidant potential in corals using the FRAP assay. *J. Exp. Mar. Biol. Ecol.*, 302: 201-211.
26. Huang, W., S. Lu, Z. Huang, X. Liu and L. Mou *et al.*, 2013. Allosteric: A method for predicting allosteric sites. *Bioinformatics*, 29: 2357-2359.
27. Case, A.J., 2017. On the origin of superoxide dismutase: An evolutionary perspective of superoxide-mediated redox signaling. *Antioxidants*, Vol. 6. 10.3390/antiox6040082.
28. Das, M.C., P. Sandhu, P. Gupta, P. Rudrapaul and U.C. De *et al.*, 2016. Attenuation of *Pseudomonas aeruginosa* biofilm formation by vitexin: A combinatorial study with azithromycin and gentamicin. *Sci. Rep.*, Vol. 6. 10.1038/srep23347.

29. Carugo, O., 2003. How root-mean-square distance (r.m.s.d.) values depend on the resolution of protein structures that are compared. *J. Appl. Crystallogr.*, 36: 125-128.
30. Patrick, G.L., 2017. *An Introduction to Medicinal Chemistry*. 6th Oxford University Press, Oxford, United Kingdom, Pages: 912.
31. Patil, R., S. Das, A. Stanley, L. Yadav, A. Sudhakar and A.K. Varma, 2010. Optimized hydrophobic interactions and hydrogen bonding at the target-ligand interface leads the pathways of drug-designing. *PLoS ONE*, Vol. 5. 10.1371/journal.pone.0012029.
32. Bissantz, C., B. Kuhn and M. Stahl, 2010. A medicinal chemist's guide to molecular interactions. *J. Med. Chem.*, 53: 5061-5084.